Development of Brake System and Regenerative Braking Cooperative Control Algorithm for Automatic-Transmission-Based Hybrid Electric Vehicles

Jiweon Ko, Sungyeon Ko, Hanho Son, Byoungsoo Yoo, Jaeseung Cheon, and Hyunsoo Kim

Abstract—In this paper, a brake system for an automatic transmission(AT)-based hybrid electric vehicle (HEV) is developed, and a regenerative braking cooperative control algorithm is proposed, with consideration of the characteristics of the brake system. The brake system does not require a pedal simulator or a fail-safe device, because a hydraulic brake is equipped on the rear wheels, and an electronic wedge brake (EWB) is equipped on the front wheels of the vehicle. Dynamic models of the HEV equipped with the brake system developed in this study are obtained, and a performance simulator is developed. Furthermore, a regenerative braking cooperative control algorithm, which can increase the regenerative braking energy recovery, is suggested by considering the characteristics of the proposed hydraulic brake system. A simulation and a vehicle test show that the brake system and the regenerative braking cooperative control algorithm satisfy the demanded braking force by performing cooperative control between regenerative braking and friction braking. The regenerative braking cooperative control algorithm can increase energy recovery of the regenerative braking by increasing the gradient of the demanded braking force against the pedal stroke. The gradient of the demanded braking force needs to be determined with consideration of the driver's braking characteristics, regenerative braking energy, and the driving comfort.

Index Terms—Cooperative control, electronic wedge brake (EWB), hybrid electric vehicle (HEV), hydraulic brake, regenerative braking.

I. INTRODUCTION

REGENERATIVE braking is a core technology for increasing the fuel efficiency of the electric vehicle (x-EV) equipped with energy storage units, such as a battery and an ultracapacitor [1]. Toyota reported that the greatest factor for an improved fuel efficiency hybrid electric vehicle (HEV) is regenerative braking, which accounts for about 35% of the total energy efficiency improvement, as evident in the Toyota Prius. Studies showed that HEVs have remarkably improved their fuel efficiencies by 30%–40% through regenerative braking [2]–[4].

However, the braking force required by a driver cannot be guaranteed through regenerative braking alone, due to various limitations, such as battery state of charge, and vehicle speed. Therefore, separate friction braking, which enables active cooperative control in response to regenerative braking, according to the braking demand of the driver and the driving state, is needed [5].

A brake-by-wire system, such as the electronic hydraulic brake (EHB) or an electric actuator, has been used in the friction brake system for regenerative braking cooperative control. For an EHB, an electronically controlled brake system, and electronic stability control, the use of an oil pump and a hydraulic control unit has been developed [6], [7]. Furthermore, a system using an electronic hydraulic servo, as well as a smart booster using an electrical booster, has been proposed [8], [9]. Electronic brakes for cooperative control, which use the x-by-wire technology, include the screw-type electronic mechanical brake (EMB) and the electronic wedge-type brake (EWB). The EMB pushes the brake pad against the brake disk using a piston, which is connected to the screw, to produce a clamping force. The EWB uses a self-reinforcing effect using a wedge, which is connected to the screw, to produce a clamping force.

The EMB and EWB are new brake types that use a motor, instead of hydraulic pressure, to generate the braking force. Thus, they respond faster and can be operated under active electronic control, which can be used to independently control the braking force of each wheel [10]–[14]. In addition, a pedal simulator is required to provide the same braking feeling as that in conventional vehicles [15], and a separate fail-safe device is required, because there is no physical connection between the driver and the brake system.

The regenerative braking cooperative control algorithm is determined by the structure of the friction brake system. Research done on the regenerative braking cooperative control algorithm include a study based on the method of increasing the energy recovery by considering the efficiencies of both the front- and rear-wheel motors for four-wheel drive (4WD) HEVs [6]; a study based on an algorithm that focuses the braking force on

J. Ko, S. Ko, H. Son, and H. Kim are with the School of Mechanical Engineering, Sungkyunkwan University, Suwon 440-746, Korea (e-mail: rapkjw@nate.com; blacksure@naver.com; hanho1014@naver.com; hskim@me.skku.ac.kr).

B. Yoo is with the Hyundai-Kia R&D Center, Hwasung 445-706, Korea (e-mail: a7ybs1@hyundai.com).

J. Cheon is with the Hyundai Mobis R&D Center, Youngin 446-912, Korea (e-mail: jaeseungcheon@mobis.co.kr).
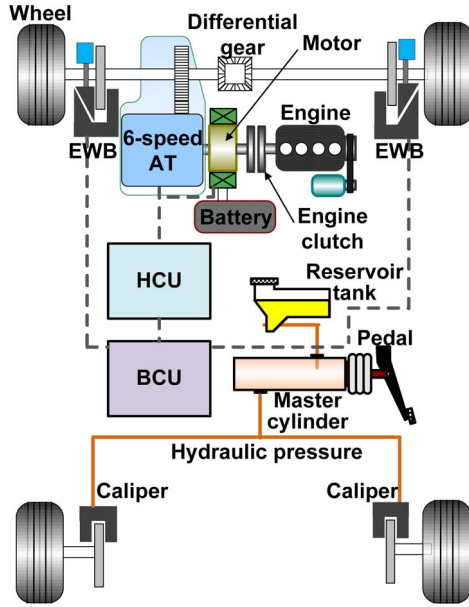
Fig. 1.   Structure of the brake system.

the front wheels to increase the energy recovery of regenerative braking of a front-wheel drive fuel cell electric vehicle [16]; and a study based on regenerative braking cooperative control, using a genetic algorithm and fuzzy control to improve vehicle stability and energy recovery [17], [18]. Another study developed an electric regenerative power-assisted brake for the cooperative control of a 4WD hybrid electric van and carried out a simulation to verify its performance [19]. Mi *et al.* proposed an electronic control brake system that integrated regenerative braking and an antilock braking system to prevent wheel lock [20].

This study proposes an electronic friction brake system for regenerative braking cooperative control that does not require a separate pedal simulator, or a fail-safe device with EWB in the front wheels, as well as a hydraulic brake in the rear wheels of an automatic transmission (AT)-based parallel-type HEV. Furthermore, a regenerative braking cooperative control algorithm, which can increase the regenerative braking energy recovery, is suggested by considering the characteristics of the proposed brake system. A dynamic model of the HEV equipped with the regenerative braking cooperative control system was obtained, and a performance simulator was developed. The performance of the regenerative braking cooperative control system was evaluated, by simulation and vehicle test.

II. STRUCTURE AND DYNAMIC MODEL OF THE BRAKE SYSTEM

A. Brake System

Fig. 1 shows the structure of the brake system that is proposed in this study. The target vehicle is a front-wheel-drive-type six-speed AT-based HEV. During braking, the front wheels perform both regenerative and friction braking, and the rear wheels perform only friction braking. The front wheels have two EWBs, whereas the rear wheels have two hydraulic brakes.

As in conventional hydraulic friction braking, the rear-wheel hydraulic brake generates a master cylinder pressure when the driver steps on the brake pedal, and this pressure is transmitted to the rear-wheel caliper through the hydraulic line, to generate a clamping force. The hybrid control unit (HCU) determines the amount of regenerative braking, according to the required regenerative braking force, determined by the brake control unit (BCU) and the gear ratio. The difference between the conventional regenerative braking cooperative control system and the newly proposed control system can be explained as follows.

The regenerative braking cooperative control algorithm needs to be determined based on the structure of the friction brake system. In the electrohydraulic four friction brakes with regenerative braking, which have been applied to existing HEVs, the friction braking force is determined from the total braking force minus the regenerative braking force at first and is then distributed to the front and rear wheels. In this system, the same braking pressure is supplied to the front and rear wheels. Then, the friction braking force of the front and rear wheels is determined by the brake design parameters, such as the caliper piston area and the effective radius of the disk. This brake system has the advantage of using conventional hydraulic brake devices, such as a master cylinder and a caliper. However, the drag force by the residual pressure in the caliper has been pointed out as a disadvantage, which decreases fuel efficiency [7].

In current technology, four EWBs for all four wheels with regenerative braking have yet to be applied to any HEV, because, in this system, the brake pedal is not physically connected to the brake, which does not meet the vehicle safety regulations. In addition, there are some problems that need to be solved, such as wedge jamming and high cost [10], [15].

The new brake system proposed in this study consists of two EWBs at the front wheel and two hydraulic brakes at the rear wheel. In the proposed new brake system, first, the rear friction braking force is determined by the pedal effort, using the hydraulic pressure, and the front demanded braking force is obtained from the total braking force minus the rear friction braking force. Then, the front friction braking force is determined from the front demanded braking force minus the regenerative braking force. The proposed brake system has such benefits as effective handling of urgent braking, due to fast response, owing to the use of EWB on the front wheel. Moreover, the proposed brake system does not require a pedal simulator and a fail-safe device since a hydraulic brake is used on the rear wheel.

B. Dynamic Modeling of the Proposed Brake System

Dynamic modeling was performed, to evaluate the performance of the brake system developed in this study.

1) Front EWB: Fig. 2 shows the EWB hardware, which is equipped on the front wheels of the subject vehicle. The operation principle of the EWB is as follows [11]: The actuator of the EWB rotates, which delivers its rotary motion to the screw, and the wedge starts its linear motion; the wedge moves diagonally and generates friction between the wedge pad and the disk.
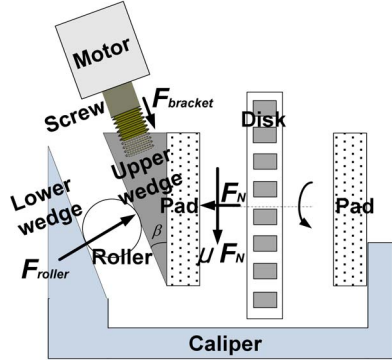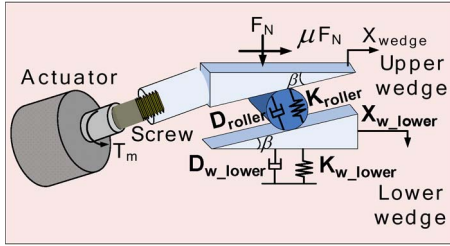
Fig. 2.   EWB.

Fig. 3.   EWB model.

In Fig. 3, the EWB model is shown. The EWB model consists of an actuator, a screw, a bracket, and a wedge [11], [21].

Wedge: The upper wedge block is modeled as a rigid body with mass, the roller as a spring damper, and the lower wedge block as both mass and a spring damper (see Fig. 3). The friction between the upper and lower wedges and that between the wedges and the roller are ignored, because they are both small. The equation of motion of the upper wedge can be derived as follows:

$$M_{\text{wedge}}\ddot{X}_{\text{wedge}} + F_{\text{roller}}\sin\beta = F_{\text{bracket}}\cos\beta + \mu F_N \quad (1)$$

$$F_{\text{bracket}} = \frac{T_m}{r_{\text{screw}}}\cdot\tan\alpha \quad (2)$$

$$F_N = F_{\text{roller}}\cdot\cos\beta + F_{\text{bracket}}\cdot\sin\beta \quad (3)$$

where M_{wedge} is the mass of the upper wedge, X_{wedge} is the parallel displacement of the upper wedge, F_{roller} is the roller force, μ is the friction coefficient between the pad and the disk, F_N is the clamping force, F_{bracket} is the force of the bracket, T_m is the actuator torque, r_{screw} is the average radius of the screw, α is the lead angle of the screw, and β is the wedge angle.
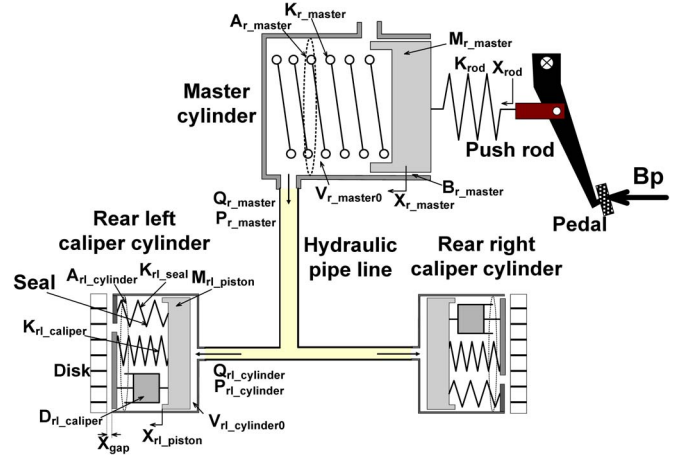

Fig. 4.   Rear hydraulic brake model.

The roller force, i.e., F_{roller}, can be determined from the compression displacement of the roller, as follows:

$$F_{\text{roller}} = K_{\text{roller}}\cdot X_{roller\_c} + D_{\text{roller}}\cdot\dot{X}_{roller\_c} \quad (4)$$

where X_{roller_c} is the compression of the roller, K_{roller} is the stiffness of the roller, and D_{roller} is the damping coefficient of the roller.

2) Rear Hydraulic Brake: Fig. 4 shows a schematic of the rear hydraulic brake. The hydraulic brake works as follows: The brake pedal displacement of the driver moves the piston of the master cylinder through the push rod to generate a braking pressure. This braking pressure is delivered to the left and right calipers of the rear wheels through the hydraulic pipeline. The pressure of the caliper cylinder pushes the piston to compress the pad to the disk, generating a braking force (see Fig. 4).

The dynamic model of the rear-wheel hydraulic brake is derived below.

Master Cylinder: The dynamic equation of the master cylinder can be derived as follows:

$$M_{r\_master}\ddot{X}_{r\_master} + B_{r\_master}\dot{X}_{r\_master}$$
$$+ K_{r\_master}X_{r\_master} + P_{r\_master}A_{r\_master} = K_{\text{rod}}X_{rod\_c} \quad (5)$$

$$\dot{X}_{rod\_c} = \dot{X}_{\text{rod}} - \dot{X}_{r\_master} = \ell\dot{B}p - \dot{X}_{r\_master} \quad (6)$$

where K_{rod} is the stiffness of the push rod, B_{r_master} is the damping coefficient of the master cylinder, K_{r_master} is the stiffness of the master cylinder return spring, M_{r_master} is the mass of the piston, A_{r_master} is the area of the piston, X_{r_master} is the displacement of the piston, X_{rod_c} is the compression of the push rod, P_{r_master} is the pressure of the master cylinder, Bp is the brake pedal stroke, and ℓ is the lever ratio that is proportional to the brake pedal stroke, i.e., Bp.

The pressure of the master cylinder is determined as follows:

$$\dot{P}_{r\_master} = \frac{\beta_{\text{oil}}}{(V_{r\_master0} - A_{r\_master}X_{r\_master})}$$
$$\times(A_{r\_master}\dot{X}_{r\_master} - Q_{r\_master}) \quad (7)$$

where $V_{r_{master0}}$ is the initial volume of the master cylinder, β_{oil} is the bulk modulus of the brake oil, and Q_{r_master} is the rate of the flow that is distributed to the left and right caliper cylinders.

Caliper: Assuming that the rates of the flows to the left and right calipers, respectively, are equal, the pressure of the caliper cylinder can be determined as follows (see Fig. 4):

$$Q_{rl\_cylinder} = \frac{1}{2}Q_{r\_master} \qquad (8)$$

$$\dot{P}_{rl\_cylinder} = \frac{\beta_{\mathrm{oil}}}{(V_{rl\_cylinder0} + A_{rl\_cylinder}X_{rl\_piston})}$$
$$\cdot (Q_{rl\_cylinder} - A_{rl\_cylinder}\dot{X}_{rl\_piston}) \qquad (9)$$

where $Q_{rl\_cylinder}$ is the rate of the flow that goes to the left caliper cylinder, $V_{rl\_cylinder0}$ is the initial volume of the caliper cylinder, $A_{rl\_cylinder}$ is the area of the caliper piston, and X_{rl_piston} is the displacement of the caliper piston.

There is a seal between the piston and the cylinder of the rear-wheel caliper. It was assumed that the reaction force of the seal acts in the opposite direction to the moving direction of the piston and is proportional to the displacement of the piston. If the piston displacement is smaller than the gap between the pad and the disk, then the reaction force of the seal is equal to the force generated by the pressure of the master cylinder, and no clamping force is generated, because the piston does not compress the pad to the disk. In this case, the reaction force of the caliper seal is represented as follows:

$$K_{rl\_seal}X_{rl\_piston} = P_{rl\_cylinder}A_{rl\_cylinder} \qquad (10)$$

where K_{rl_seal} is the stiffness of the seal. If the piston displacement becomes greater than the gap and compresses the pad to the disk, then the dynamic equation of the caliper is as follows:

$$X_{rl\_piston\_c} = X_{rl\_piston} - X_{\mathrm{gap}} \qquad (11)$$

$$M_{rl\_piston}\ddot{X}_{rl\_piston} + K_{rl\_seal}X_{rl\_piston}$$
$$+ D_{rl\_caliper}\dot{X}_{rl\_caliper\_c} + K_{rl\_caliepr}X_{rl\_caliper\_c}$$
$$= P_{rl\_cylinder}A_{rl\_cylinder} \qquad (12)$$

$$F_{rl\_clamping} = D_{rl\_caliper}\dot{X}_{rl\_caliper\_c}$$
$$+ K_{rl\_caliepr}X_{rl\_caliper\_c} \qquad (13)$$

where M_{rl_piston} is the mass of the caliper piston, $F_{rl\_clamping}$ is the clamping force, $X_{rl\_caliper\_c}$ is the compression of the caliper, X_{gap} is the gap between the pad and the disk, $K_{rl\_caliper}$ is the stiffness of the caliper, and $D_{rl\_caliper}$ is the damping coefficient of the caliper.

III. REGENERATIVE BRAKING COOPERATIVE CONTROL ALGORITHM

Fig. 5 shows the regenerative braking cooperative control algorithm proposed in this study, which distributes the friction braking force and the regenerative braking force. The
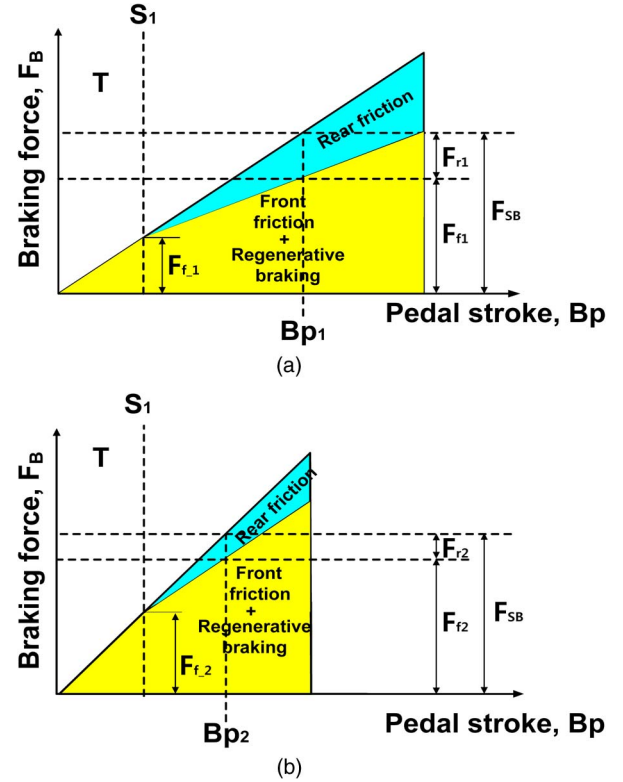

Fig. 5. Regenerative braking cooperative control algorithm.

demanded braking force F_B at braking is determined according to the brake pedal stroke, i.e., Bp. In this paper, the demanded braking force F_B is represented as

$$F_B = Bp \cdot g \qquad (14)$$

where g is the gradient of the total demanded braking force to the pedal stroke, i.e., $g = dF_B/dBp$.

The demanded braking force F_B is supplied by the summation of the front and rear braking forces as

$$F_B = F_f + F_r \qquad (15)$$

where F_f is the front braking force, and F_r is the rear braking force.

In Fig. 5(a), the braking force distribution map is shown for the gradient, i.e., $dF_B/dBp = g_1$. In the brake system proposed in this study (see Fig. 1), the rear braking force F_r is generated by the caliper cylinder pressure, which is proportional to the brake pedal stroke Bp. However, as described in (10)–(13), the rear braking force F_r is generated only when the cylinder piston displacement becomes greater than the gap, i.e., X_{gap}. If we define the brake pedal stroke, which is equivalent to X_{gap}, as S_1, F_r is not generated until S_1 (region T). The S_1 value can be determined from a vehicle test or from a simulation. In the vehicle test, S_1 can be obtained as the pedal stroke where the deceleration occurs, which can be measured by the acceleration sensor. In the simulation, S_1 is determined as the pedal stroke where the rear clamping force is generated.
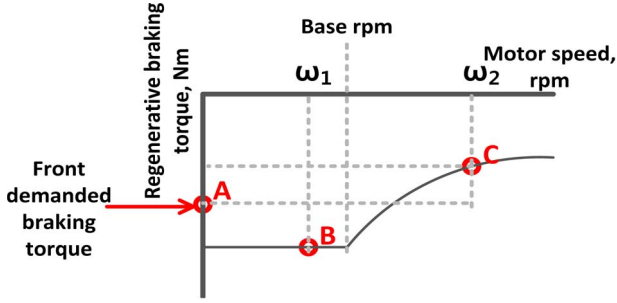
Fig. 6. Drive motor characteristic map.

The front braking force F_f is composed of the friction braking force $F_{f\_friction}$ and the regenerative braking force F_{regen} as

$$F_f = F_{f\_friction} + F_{regen}. \qquad (16)$$

If the regenerative braking force F_{regen} can singularly supply F_f, then the front-wheel braking will be performed only by the regenerative braking. If F_{regen} is smaller than F_f, then both regenerative braking and friction braking are performed. The regenerative braking force F_{regen} can be determined from a motor characteristic map (see Fig. 6) according to vehicle speed, i.e., motor speed. As shown in Fig. 6, the maximum regenerative braking torque remains the same under the motor base r/min and decreases when the motor speed increases. At the motor speed of ω_1, if the front demanded braking torque (A) is smaller than the maximum regenerative braking torque (B), the front-wheel braking will be performed only by regenerative braking. At the motor speed of ω_2, since the maximum regenerative braking torque (C) is smaller than the front demanded braking torque (A), the demanded braking torque cannot be supplied by only regenerative braking. In this case, the insufficient braking torque of the front wheel needs to be supplemented with front friction braking.

To maximize the energy recovery through regenerative braking, the braking force must be distributed, such that the braking force of the front wheels performing regenerative braking is maximized. This can be achieved by increasing gradient g. Fig. 5(b) shows the braking force distribution for the increased gradient, i.e., g_2. It is noted in Fig. 5(b) that the front braking area increases when Bp is equal to S_1, compared with that in the case of $g_1(F_{f\_1} > F_{f\_2})$, which increases the regenerative braking force. However, since the pedal stroke decreases from Bp_1 to Bp_2 for the same demanded braking force (F_{SB}), a sensitive brake pedal feeling is expected. In addition, since rear braking force F_r is proportional to the pedal stroke [see (5) and (6)], F_r would also decrease from F_{r1} to F_{r2} for the same F_{SB}; hence, the front wheels will require greater braking force $(F_{f2} > F_{f1})$ [see (15)].

Fig. 7 shows the braking force distribution for g_1 and g_2. In the case of g_1, braking is performed with the front wheels only, through the braking force of the front wheels F_{f_1} until deceleration D_1. If the deceleration becomes greater than D_1, then braking will be performed with both front and rear wheels. In the case of g_2, braking is performed with the front wheels only, through the braking force of the front wheels F_{f_2} until deceleration D_2. If the deceleration becomes greater than D_2, then braking will be performed with both front and rear wheels.
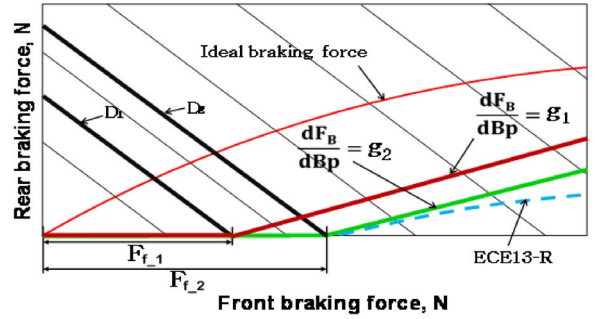

Fig. 7. Braking force distribution by the regenerative braking cooperative control algorithm.

To ensure the braking safety of the vehicle, the United Nations Economic Commission for Europe established a regulation (ECE13-R) that strictly regulates the distribution range of the braking forces between the front and rear wheels. It is shown in Fig. 7 that the braking force distribution for g_1 and g_2 satisfies ECE13-R.

IV. REGENERATIVE BRAKING PERFORMANCE SIMULATOR

A. Powertrain Model

A simulator was developed to evaluate the performances of the brake system and the regenerative braking cooperative control algorithm proposed in this study. During regenerative braking, the engine clutch is disengaged. Therefore, only the motor and transmission were modeled, which are the powertrain elements used in regenerative braking.

Motor: The motor receives voltage and current from the battery. It is used not only as a motor during driving but also as a generator during regenerative braking. The motor was modeled as a first-order system, using the characteristic curve and the performance map shown as follows:

$$\frac{T_{motor}}{T_{motor\_desired}} = \frac{1}{1 + \tau_{motor} \cdot s} \qquad (17)$$

$$\omega_{motor} = \frac{V_h N_f N_{AT}}{R_t} \qquad (18)$$

where T_{motor} is the actual motor torque, $T_{motor\_desired}$ is the desired motor torque, T_{motor} is the time constant of the motor, ω_{motor} is the motor speed, V_h is the vehicle speed, N_f is the final reduction gear ratio, and N_{AT} is the AT gear ratio.

Automatic Transmission: The six-speed AT consists of two single-pinion planetary gears and one double-pinion planetary gear. The operative elements are two wet multiple disk clutches, three wet multiple disk brakes, and a one-way clutch (see Fig. 8).

Vehicle: A vehicle dynamic model was constructed, using CarSim software. The CarSim vehicle model can be built in characterizing vehicles and their behavior reproduced with mathematical models. The CarSim vehicle model covers the complete vehicle system and its inputs from the driver, ground, and aerodynamics. The models are extensible, using MATLAB/ Simulink to add advanced controllers or component models, such as tires, brakes, powertrain, etc. [22].
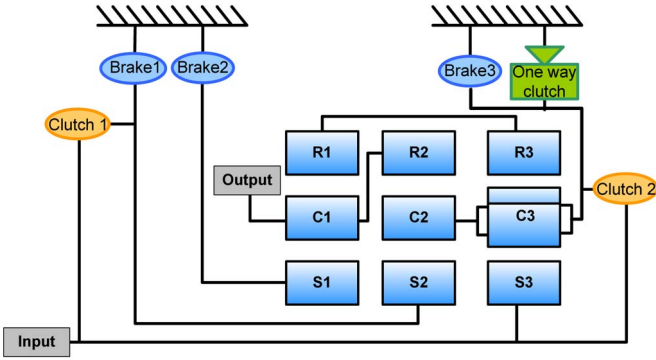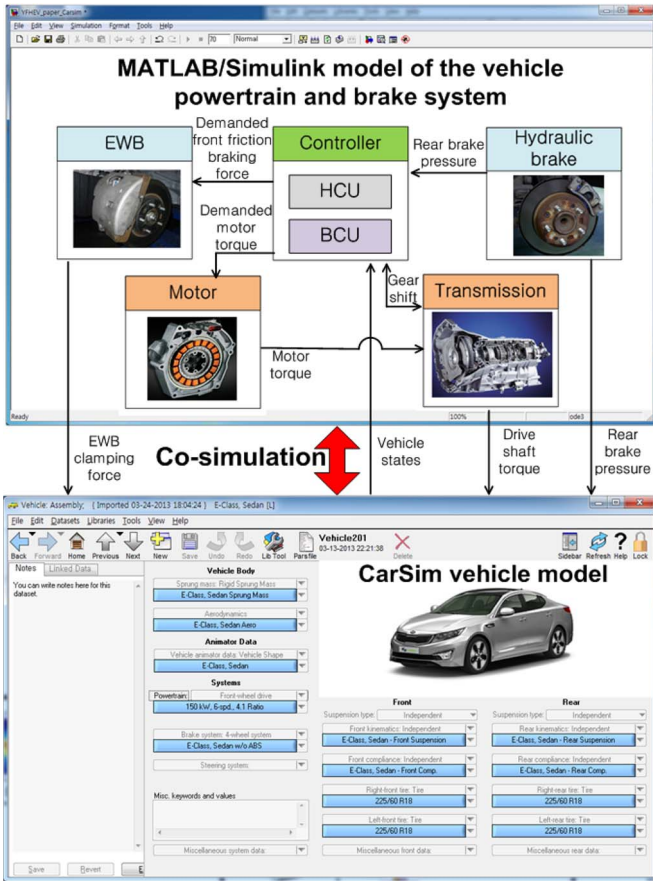
Fig. 8. Schematic of a six-speed AT.

Fig. 9. Regenerative braking performance simulator.

B. Regenerative Braking Performance Simulator

A regenerative braking performance simulator was developed, by combining the MATLAB/Simulink model of the EWB, hydraulic brake, powertrain, and the CarSim vehicle model (see Fig. 9). The cosimulation using the MATLAB/Simulink model and the CarSim model is performed as follows.

The pedal stroke and the pressure calculated from the rear hydraulic brake model are input to the BCU of the controller. The BCU determines the total demanded braking torque according to the pedal stroke and calculates the rear brake torque. The front demanded braking torque is determined from the total demanded braking torque minus the rear brake torque. The front demanded braking torque is sent to the HCU of the controller, and then, the HCU determines the regenerative braking motor

TABLE I
VEHICLE PARAMETERS

| Vehicle parameters		
Vehicle	Gross vehicle weight	2050 kg
	Wheel base	2.8 m
	Drag coefficient	0.3
	Tire radius	0.32 m
Engine	Stroke volume	2359 cc
	Maximum torque	198 Nm
Motor	Power	30 kW
	Maximum speed	6500 rpm
	Maximum torque	215 Nm
Battery	Total voltage	270 V
	Capacity	5.3 Ah
AT	Gear ratio	1st gear: 4.2
		2nd gear: 2.6
		3rd gear: 1.8
		4th gear: 1.4
		5th gear: 1.0
		6th gear: 0.8
	Final reduction gear ratio	3.3
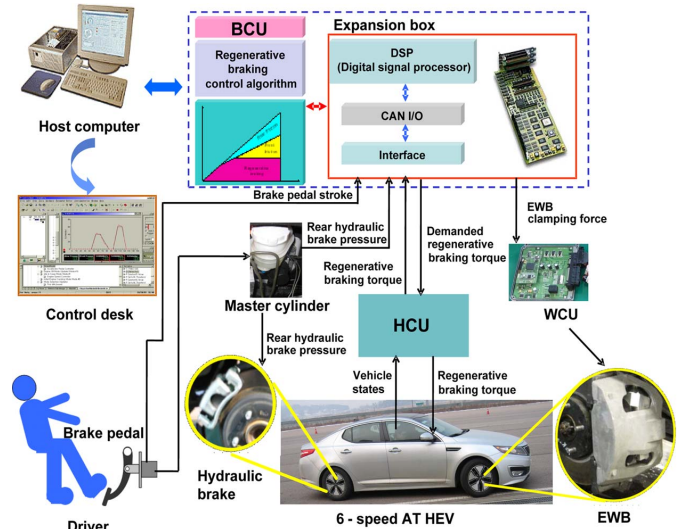
Fig. 10. Configuration of the vehicle test apparatus.

torque and the EWB front friction braking force, considering the vehicle conditions (gear step and vehicle speed). The drive shaft torque from the transmission model, the clamping force from the EWB model, and the brake pressure from the hydraulic brake model are sent to the CarSim vehicle model. The vehicle parameters are shown in Table I.

V. VEHICLE TEST

To evaluate the performance of the proposed brake system and the regenerative braking cooperative control algorithm, a vehicle test was performed, with a six-speed AT-based HEV. Fig. 10 shows the configuration of the vehicle test apparatus. The regenerative braking cooperative control algorithm composed of the MATLAB/Simulink was installed in the host PC, which used a digital signal processor and CAN I/O to act as the BCU.

When a driver steps on the brake pedal, the sensor signal of the brake pedal stroke and the pressure of the rear-wheel master cylinder are sent to the BCU, and the braking pressure generated from the rear-wheel master cylinder pushes the

piston of the rear-wheel caliper to ultimately generate a friction braking force for the rear wheels. The BCU determines the total demanded braking torque according to the pedal stroke and calculates the rear-wheel braking torque, as well as the front demanded braking torque, using the pressure generated from the rear-wheel master cylinder. The front demanded braking torque is sent to the HCU, and the HCU determines the regenerative braking torque from the vehicle conditions and then sends it to the BCU. The BCU converts the front demanded braking torque, minus the regenerative braking torque, to the demanded clamping force and sends it to the wedge control unit, which makes the EWB generate a clamping force.

VI. SIMULATION AND VEHICLE TEST RESULTS

The performance of the brake system and the regenerative braking cooperative control algorithm developed in this study were evaluated by simulation and a vehicle test. The braking simulation and test were carried out at the deceleration of 0.2 g from 100 km/h, since in the FTP75 driving mode, braking is mostly performed at a deceleration below 0.2 g.

A. Simulation and Vehicle Test Results for $dF_B/dBp = g_1$

Fig. 11 shows the simulation and the vehicle test results, when the gradient of the braking force against the pedal stroke was $dF_B/dBp = g_1$. In the simulation results, the brake pedal stroke (b) starts to increase at t = 1 s and is maintained constant at 38 mm. The pressure of the master cylinder starts to increase together with the brake pedal stroke and is maintained constant at 10.4 bars. The vehicle speed (a) begins to decrease from 100 km/h and becomes zero at 14 s. Once braking is started, the gear step of the AT (c) decreases from fifth to fourth and to third and maintains the first gear when the vehicle speed becomes 9 km/h or lower. During regenerative braking, the gear shift of the target HEV is performed, according to the brake pedal stroke and vehicle speed, as conventional AT. The front demanded braking torque (d) increases in proportion to the brake pedal stroke and stays constant at 855 Nm. The regenerative braking wheel torque (d) occurs in section R and increases in sections S and P. It increases according to the motor characteristics, with the decrease in vehicle speed (motor speed). In section Q, the regenerative braking wheel torque is equal to the front demanded braking torque. The rear friction braking torque (d) does not appear in section R, even when the pedal stroke increases, because the piston displacement is smaller than the gap between the pad and the disk. In section S, a rear friction braking torque (d) is generated, increased, and then maintained constant at 262 Nm. The EWB clamping force (e) increases in sections R and S to meet the front demanded braking torque because the regenerative braking torque is insufficient (d), and decreases in section P, as the regenerative braking torque increases. In section Q, no EWB clamping force is generated, because only the regenerative braking is used for the front wheels. The deceleration (f) increases in the negative direction as the brake pedal stroke increases, until it becomes constant at 0.2 g. The energy (g) recovered from regenerative braking is 297 KJ.
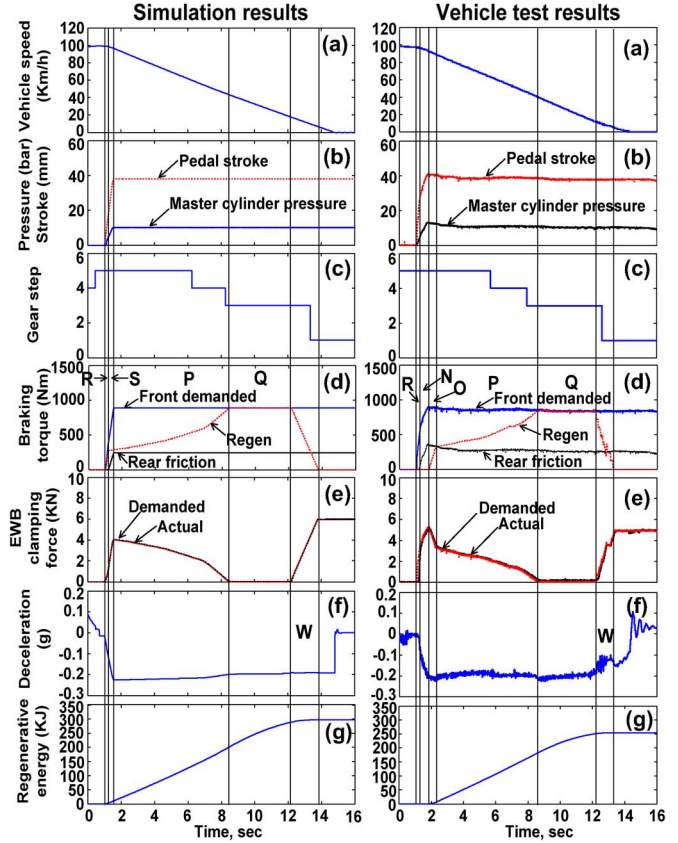

Fig. 11. Simulation and vehicle test results for $dF_B dBp = g_1$.

The vehicle test results in Fig. 11 show almost the same behaviors as the simulation results. The test results of the brake pedal stroke, master cylinder pressure (b), and gear step (c) are almost identical with the simulation results. The difference in the gear shift time (c) is due to the small difference in the pedal stroke and vehicle speed, between the simulation and the test. The regenerative braking wheel torque (d) begins to increase in section O, whereas the regenerative braking wheel torque of the simulation occurs as soon as the braking starts at R. This is because it takes a certain amount of time for the conversion of the vehicle operation mode from the driving mode to the regenerative braking mode, during which the state of the battery changes to a rechargeable state, as well as time for the engine to stop operating. In section N, a rear friction braking torque (d) is generated, increased, and maintained almost constant at 274 Nm during braking. The EWB clamping force (e) increases in sections R and N, showing a higher value than the simulation result, because there is no regenerative braking torque in this region. The deceleration (f) increases in the negative direction, as the brake pedal stroke increases, until it becomes constant at 0.2 g. The deceleration fluctuates in section W, whereas the deceleration in the simulation results seems quite smooth. This can be explained as follows: Section W is the transient region where regenerative braking decreases and friction braking begins to increase. As shown in the vehicle test results, it is found that the regenerative braking wheel torque decreases in a small stepwise manner, due to the signal processing characteristic of the measurement device at low vehicle speed. However, since the EWB clamping force cannot be controlled
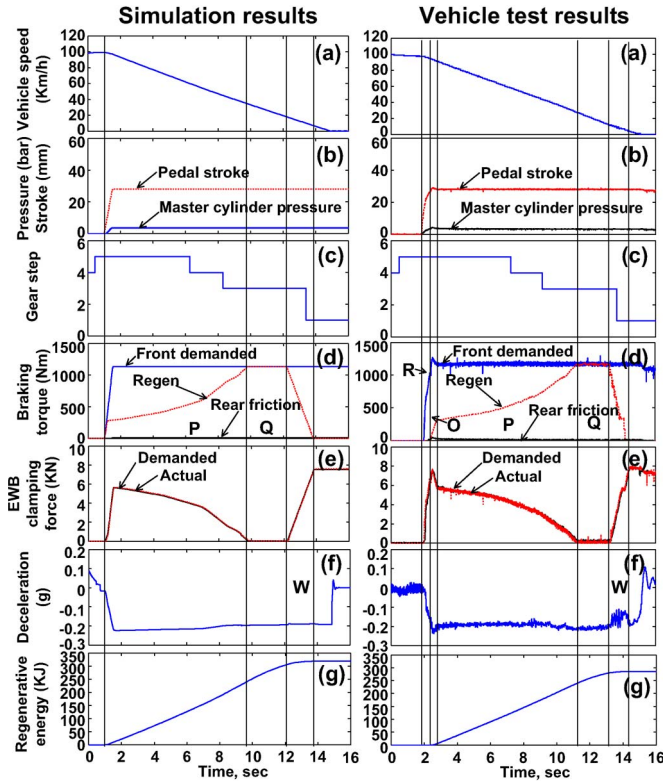
Fig. 12.   Simulation and vehicle test results for $dF_B/dBp = g_2$.

to compensate the stepwise change in the regenerative braking wheel torque, deceleration fluctuation occurs. The energy (g) recovered from regenerative braking is 254 KJ, which is less than that in the simulation results (297 KJ). This is because in the simulation, a regenerative braking wheel torque is generated as soon as the brake pedal stroke increases, whereas in sections R and N of the vehicle test results, no regenerative braking wheel torque is generated, due to the conversion time of the vehicle operation mode.

B. Simulation and Vehicle Test Results for $dF_B/dBp = g_2$

Fig. 12 shows the simulation and the vehicle test results, when the gradient of the braking force is increased to $dF_B/dBp = g_2$. In the simulation results, the brake pedal stroke (b) starts to increase at t = 1 s and then stays constant at 28 mm. The pressure of the master cylinder starts to increase together with the brake pedal stroke and then stays constant at 3.3 bars. For the same demanded deceleration, i.e., 0.2 g, the pedal stroke and rear braking pressure are smaller than those at $dF_B/dBp = g_1$; hence, greater braking torque (force) is needed for the front wheels [see Fig. 5(b)]. Therefore, the front demanded braking torque (d) increases in proportion to the pedal stroke and stays constant at 1133 Nm, which is greater than that of $dF_B/dBp = g_1$. Regenerative braking wheel torque (d) occurs and increases in section P. In section Q, it stays constant, which is greater than that of $dF_B/dBp = g_1$, because it is equal to the front demanded braking torque. The rear friction braking torque (d) is almost zero. This is because the pressure of the rear master cylinder is smaller than the threshold value (3.5 bars), which is the pressure where the caliper piston starts to compress the pad to the disk, and because there is a

gap between the pad and the disk. The EWB clamping force (e) begins to increase, as soon as the braking starts. It decreases in section P, as the regenerative braking torque increases. The EWB clamping force is zero, since only regenerative braking is used for the front wheels, in section Q. The deceleration (f) increases in the negative direction, as the brake pedal stroke increases, and then, it becomes constant at 0.2 g. Since the gradient of the braking force is greater, the regenerative braking area becomes larger, and the recovered energy (g) is 318 KJ, which is greater than 297 KJ at $dF_B/dBp = g_1$.

The vehicle test results in Fig. 12 show almost the same behaviors as the simulation results. The test results of the brake pedal stroke, master cylinder pressure (b), and gear step (c) are almost identical to the simulation results. The gear shift of the HEV is performed according to the brake pedal stroke and vehicle speed. The difference in the gear shift time for g_1 (see Fig. 11) and g_2 (see Fig. 12) is due to the difference in the brake pedal stroke, although the vehicle speeds are almost the same. The front demanded braking torque (d) increases in proportion to the brake pedal stroke and then stays constant at 1190 Nm, which is greater than that in the case of $dF_B/dBp = g_1$. The regenerative braking wheel torque (d) occurs in section O and increases in section P. In section Q, it is greater than that of $dF_B/dBp = g_1$. The rear friction braking torque (d) is almost zero, since the pedal stroke is smaller than the gap. The EWB clamping force (e) of the test results shows a high peak in sections R and O to meet the front demanded braking torque because the regenerative braking wheel torque is not generated in section R. The EWB clamping force decreases as the regenerative braking wheel torque increases. The deceleration (f) increases in the negative direction as the brake pedal stroke increases until it becomes constant at 0.2 g. The deceleration (f) shows a fluctuation in the transient region (W), where regenerative braking and friction braking cross, for the same reason previously explained. The recovered energy (g) is 287 KJ, which is greater than 254 KJ at $dF_B/dBp = g_1$.

From the simulation and vehicle test results in Figs. 11 and 12, it is found that the brake system and the regenerative braking cooperative control algorithm developed in this study satisfy the demanded braking force by applying regenerative braking and friction braking. The hydraulic brake system at the rear wheels is beneficial for energy recovery, because there is an initial region of the brake pedal stroke where only regenerative braking can be used, due to the characteristics of the seal. In the regenerative braking cooperative control algorithm (see Fig. 5), the pedal stroke for the same demanded deceleration (braking force) decreases, as well as the pressure of the master cylinder, as the gradient of the total demanded braking force for the pedal stroke increases. This provides an increase in the front demanded braking force, the maximum torque of regenerative braking, and the recovered energy. However, if the gradient excessively increases, the braking force will considerably vary, even with minor changes in the pedal stroke. As a result, driving comfort can deteriorate by the sensitive braking. Therefore, the gradient of the total demanded braking force for the pedal stroke must be appropriately designed by considering the driver's braking characteristics, the amount of energy recovered through regenerative braking, and the driving comfort.

VII. Conclusion

In this paper, a brake system for an AT-based HEV has been developed, and a regenerative braking cooperative control algorithm has been proposed, with consideration of the characteristics of the brake system. The proposed brake system does not require a pedal simulator or a fail-safe device, because a hydraulic brake is equipped on the rear wheels, and an EWB is equipped on the front wheels. To evaluate the performance of the brake system and the regenerative braking cooperative control algorithm proposed in this study, dynamic models of the EWB, the rear-wheel hydraulic brake, and the HEV powertrain of the subject vehicle were constructed, and a regenerative braking performance simulator was developed, using the cosimulation of the MATLAB/Simulink-powertrain and brake system model and the CarSim vehicle model. A simulation and a vehicle test were performed to evaluate the performance of the proposed brake system and the regenerative braking cooperative control algorithm.

The simulation and vehicle test results showed that the brake system and the regenerative braking cooperative control algorithm developed in this study satisfied the demanded braking force, by distributing the regenerative braking force and friction braking force, with consideration of the characteristics of the brake system. If the pedal stroke is smaller than the threshold value, rear braking is not performed, and braking is performed only by regenerative braking or by regenerative braking and friction braking at the front wheels. If the pedal stroke is larger than the threshold value, braking is performed by regenerative braking at the front wheels and friction braking at the rear wheels or by regenerative braking and friction braking at the front wheel and friction braking at the rear wheels.

When the gradient of the total demanded braking force against the pedal stroke was increased, the rear-wheel friction braking force became smaller, and more braking force was distributed to the front wheels, thus increasing the energy recovery of regenerative braking. However, if the gradient of the total demanded braking force for the pedal stroke becomes too large, driving comfort can be degraded due to the sensitive brake pedal feeling. Therefore, the gradient of the total demanded braking force against the pedal stroke needs to be appropriately determined by considering the amount of energy recovered through regenerative braking and driving comfort.

References

[1] D. Antanaitis, "Effect of regenerative braking on foundation brake performance," Soc. Autom. Eng., Warrendale, PA, USA, SAE Tech. Paper 2010-01-1681, 2010.

[2] T. Yaegashi, S. Sasaki, and T. Abe, "Toyota hybrid system: Its concept and technology," presented at the FISITA World Autom. Congr., Paris, France, 1998, F98TP095.

[3] K. Yamaguchi, S. Maroto, K. Kobayshi, M. Kawamoto, and Y. Miyaishi, "Development of a new hybrid system-dual system," Soc. Autom. Eng., Warrendale, PA, USA, SAE Tech. Paper 960231, 1996.

[4] M. Panagiotidis, G. Delarammatikas, and D. Assanis, "Development and use of a regenerative braking model for a parallel hybrid electric vehicle," Soc. Autom. Eng., Warrendale, PA, USA, SAE Tech. Paper 2000-01-0995, 2000.

[5] A. Walker, M. Lamperth, and S. Wilkins, "On friction braking demand with regenerative braking," Soc. Autom. Eng., Warrendale, PA, USA, SAE Tech. Paper 2002-01-2581, 2002.

[6] M. Soga, M. Shimada, J. Sakamoto, and A. Otomo, "Development of vehicle dynamics management system for hybrid vehicle: ECB system for improved environmental and vehicle dynamic performance," *JSAE Rev.*, vol. 23, no. 4, pp. 459–464, Oct. 2002.

[7] M. Park, S. Kim, L. Yang, and K. Kim, "Development of the control logic electronically controlled hydraulic brake system for hybrid vehicle," Soc. Autom. Eng., Warrendale, PA, USA, SAE Tech. Paper 2009-01-1215, 2009.

[8] N. Fujiki, Y. Koike, Y. Itou, G. Suzuki, and S. Goto, "Development of an electrically-driven intelligent brake system for EV," Soc. Automot. Eng., Warrendale, PA, USA, SAE Tech. Paper 2011-39-7211, 2011.

[9] H. Yeo, C. Koo, W. Jung, D. Kim, and J. Cheon, "Development of smart booster brake system for regenerative brake cooperative control," Soc. Automot. Eng., Warrendale, PA, USA, SAE Tech. Paper 2011-01-2356, 2011.

[10] J. Cheon, "Brake by wire system configuration and functions using front EWB (Electric Wedge Brake) and rear EMB (Electric-Mechanical Brake) actuators," Soc. Automotive Eng., Warrendale, PA, USA, SAE Tech. Paper 2010-01-1708, 2010.

[11] C. Jo *et al.*, "Design and control of an upper-wedge-type electronic brake," *Proc. Inst. Mech. Eng., D, J. Autom. Eng.*, vol. 224, no. 11, pp. 1393–1405, Nov. 2010.

[12] J. Kim, M. Kim, and J. Kim, "Developing of electronic wedge brake with cross wedge," Soc. Autom. Eng., Warrendale, PA, USA, SAE Tech. Paper 2009-01-0856, 2009.

[13] R. Hoseinnezhad, A. Bab-Hadiashar, and T. Rocco, "Real-time clamp force measurement in electromechanical brake calipers," *IEEE Trans. Veh. Technol.*, vol. 57, no. 2, pp. 770–777, Mar. 2008.

[14] C. Jo, S. Hwang, and H. Kim, "Clamping-force control for electromechanical brake," *IEEE Trans. Veh. Technol.*, vol. 59, no. 7, pp. 3205–3212, Sep. 2010.

[15] J. Lee, S. Woo, H. Lee, E. Park, and K. Kim, "Development of pedal module for brake-by wire," in *Proc. KSME Conf.*, Seoul, Korea, 2009, pp. 343–347.

[16] J. Ko, J. Kim, D. Hyun, and H. Kim, "Analysis of EWB performance for fuel cell electric vehicle during regenerative braking," in *Proc. KSAE Conf.*, Daegu, Korea, 2010, pp. 2960–2965.

[17] J. Guo, J. Wang, and B. Cao, "Application of genetic algorithm for braking force distribution of electric vehicles," in *Proc. 4th IEEE ICIEA Conf.*, 2009, pp. 2150–2154.

[18] D. Peng, J. Zhang, and Y. Zhang, "Regenerative braking control system improvement for parallel hybrid electric vehicle," in *Proc. ITIC*, 2006, pp. 1902–1908.

[19] A. Hartavi *et al.*, "Electric regenerative power assisted brake algorithm for front and rear wheel drive parallel hybrid electric commercial van," Soc. Autom. Eng., Warrendale, PA, USA, SAE Tech. Paper 2008-01-2606, 2008.

[20] C. Mi, H. Lin, and Y. Zhang, "Iterative learning control of antilock braking of electric and hybrid vehicles," *IEEE Trans. Veh. Technol.*, vol. 54, no. 2, pp. 486–494, Mar. 2005.

[21] J. Ko, S. Ko, I. Kim, D. Hyun, and H. Kim, "Co-operative control for regenerative braking and friction braking to increase energy recovery without wheel lock," *Int. J. Autom. Technol.*, vol. 15, no. 2, pp. 253–262, Mar. 2014.

[22] Mechanical Simulation Website 2013. [Online]. Available: http://www.carsim.com/products/carsim/index.php

Jiweon Ko received the B.S. degree in mechanical engineering from Sungkyunkwan University, Suwon, Korea, in 2009, where he is currently working toward the Ph.D. degree.

His research interests include the modeling of electronic brake systems and controls of regenerative braking for x-EVs.

Sungyeon Ko received the B.S. and M.S. degrees in mechanical engineering from Sungkyunkwan University, Suwon, Korea, in 2010 and 2012, where he has been working toward the Ph.D. degree.

His research interests include the modeling and control of in-wheel vehicles.

Hanho Son received the B.S. degree in mechanical engineering from Sungkyunkwan University, Suwon, Korea, in 2013, where he is currently working toward the M.S. degree.

His research interests include the modeling and control of plug-in hybrid electric vehicles.

Jaeseung Cheon received the Ph.D. degree in mechanical engineering from the Korea Advanced Institute of Science and Technology, Daejeon, Korea, in 2003.

Since 2004, he has been with MOBIS, engaged in the development of advanced brake systems and in-wheel motor systems. He is currently the Chief Engineer of the Brake System Design Team.

Byoungsoo Yoo received the B.S. degree in mechanical engineering from Inha University, Incheon, Korea, in 1988.

Since 1990, he has been with the chassis engineering team at the Hyundai-Kia R&D Center, Hwaseong, Korea. His research interests include the design of brake systems.

Hyunsoo Kim received the B.S. degree from Seoul National University, Seoul, Korea, in 1977; the M.S. degree from the Korea Advanced Institute of Science and Technology, Seoul, in 1979; and the Ph.D. degree from the University of Texas at Austin, Austin, TX, USA, in 1986, all in mechanical engineering.

Since 1986, he has been a Professor, Chairman, and Dean of the College of Engineering with Sungkyunkwan University, Seoul. He has authored numerous journal papers and patents. His main research interests include hybrid electric vehicle (HEV) transmission system design, regenerative braking, optimal power-distribution algorithms for HEVs, and vehicle stability control for HEVs and in-wheel vehicles.

Dr. Kim has served as a Division President of the Electric Drive Vehicle of the Korea Society of Automotive Engineers and as an Editor for the *International Journal of Automotive Technology*.